Theoretical Investigation of Structural, Optoelectronic and Thermodynamic Prpperties of Chalcogenides Based Magnesium

Y. Megdoud[a,b], Y. Benkrima[g*], L. Tairi[b,c], A. Lakel[d], S. Djellab[b,e], H. Meradji[b], S. Ghemid[b] and R. Meneceur[f],

[a]*Institute of Sciences, University Center of Tipaza- Morsli Abdallah-, Algeria*

[b]*LPR Laboratory, Département of Physics, Faculty of Science, Badji Mokhtar University, Annaba, Algeria.*

[c]*Research Center in Industrial Technologies CRTI, P.O. Box 64, Cheraga16014 Algiers Algeria*

[d]*Laboratory of Metallic and Semiconducting Materials, University of Biskra, BP 145 RP, 07000 Biskra, Algeria.*

[e]*Physics department, Faculty of Sciences ,Skikda University , Algeria.*

[f]*Unit for the Development of Renewable Energies in Arid Zones (UDERZA), El Oued University, Algeria*

[g]*Ecole Normale Supérieure de Ouargla, 30000 Ouargla, Algeria*

***Corresponding Author: megdoud.yousra@cu-tipaza.dz**

Received 10/ 06/ 2023; accepted 02/09/ 2023; Published 11/09/2023

Abstract

The structural, electronic, optical and thermodynamic properties of **$MgSe_xTe_{1-x}$**ternary mixed crystals have been studied using the ab initio full-potential linearized augmented plane wave **(FP-LAPW)** method within density functional theory **(DFT).** In this approach, the **Perdew–Burke–Ernzerhof**-generalized gradient approximation (**PBE-GGA**)was used for the exchange-correlation potential. Moreover, the recently proposed **modified Becke Johnson** (**mBJ**) potential approximation, which successfully corrects the band-gap problem was also used for band structure calculations. The ground-state properties are determined for the wurtzite bulk materials **MgTe, MgSe** and their mixed crystals at various concentrations (**x = 0.25, 0.5 and 0.75**)in the wurtzite phase. The effect of composition on lattice constant, bulk modulus and band gap was analyzed. Deviation of the lattice constant from Vegard's law and the bulk modulus from linear concentration dependence (**LCD**) were observed for the ternary **$MgSe_xTe_{1-x}$** alloys. The

microscopic origins of the gap bowing were explained by using the approach of Zunger and co-workers. On the other hand, the thermodynamic stability of these alloys was investigated by calculating the excess enthalpy of mixing, ΔHm as well as the phase diagram. It was shown that these alloys are stable at high temperature. For the optical properties, the compositional dependence of the refractive index and the dielectric constant was studied.

Keywords: *DFT, MgTe, MgSe, chalcogenides, band gap, optical properties, thermodynamic properties.*

PACS:71.15.Mb, 73.61.Cw

Tob Regul Sci. ™ 2023;9(1): 4920 - 4940
DOI: doi.org/10.18001/TRS.9.1.342

1. Introduction

Magnesium chalcogenides **MgSe** and **MgTe** are wide band gap semiconductors, which have immense technological importance due to their numerous applications in optoelectronic and luminescent devices **[1-8].**The valence band of Mg (**belonging to II-A in the periodic table**) based ternary chalcogenides does not contain a metallic d band; that makes their properties different from those of II-B compound semiconductors. The absence of a metallic d band in Mg based chalcogenides lowers the valence band maxima and results in increasing their fundamental band gaps compared to group II-B compound semiconductors. These larger band gaps of **Mg** containing II-VI compounds show that these materials are very important for devices in the completely visible range **[9].** In addition, group IIB compound semiconductors are preferably tetrahedral structures, due to tight bonding of the imperfect d orbital screening **[10];** while group IIA elements favor the rock salt structure, **MgS** and **MgSe** have the Zinc blende phase (ZB) **[11].**Although **MgTe** normally has the wurtzite phase **[12],** it is possible to grow MgTe in the ZB phase under appropriate conditions **[13, 14].** They have been extensively studied both experimentally and theoretically in rocksalt (B1), zinc blende (B3) and wurtzite (B4) crystallographic phases [15-24].Under ambient conditions, **MgSe** crystallize in the B1 structure **[15, 16].** Experimental studies show that **MgTe** crystallizes stably in the B4 structure under ambient conditions **[16-20]** and transform to NiAs (B8) structure under the application of high pressure. The normal structure of **MgTe** is wurtzite**[25],** while for **MgSe** it is zinc blende **[26].** From a theoretical point of view, **Gokoglu et al. [23];** attributed B1 structure to MgSe and B8 to MgTe using projector augmented wave method, whereas **Drief et al.**[24],suggested B1 as the most stable structure for all of MgSe and MgTe using the full potential linear augmented plane wave (FP-LAPW) method. **F El Haj Hassan et al[27];** was applied to study the structural, electronic and thermodynamic properties of MgS_xSe_{1-x}, $MgS_xTe_{1-x}$and $MgSe_xTe_{1-x}$ ternary alloys. **Imad Khan et al[28],** was studied Transition from optically inactive to active Mg-chalcogenides. Magnesium chalcogenides Due to large variation (e.g., E_g (**MgS**) = **2.56 eV** and E_g(**MgTe**) = **0.38 eV[29];** in the indirect energy band gaps of binary magnesium chalcogenides,

band gap tailoring by alloying two of these materials might be an effective approach that can yield electronic and optical properties intermediate or entirely different from the constituent binary compounds. For example, some reports on the interesting transition of band gap type (direct ↔ indirect) between the binary compounds and their ternary alloys are in Refs.**[30, 31]**:in case of magnesium chalcogenides. Using the FP-LAPW method within the **DFT** in the framework of GGA and mBJ, we investigated the phase stability, pressure-induced phase transition, structural and electronic properties of Mgs,**MgSe** and **MgTe** compounds. A summary of our results is as follows: at zero pressure, the wurtzite phase is found to be the most stable for **MgSe** and **MgTe** compounds while for **MgS** the rock salt phase is the most stable **[32].**In this paper we studied $MgSe_xTe_{1-x}$, alloy as well as the structural, electronic, optical, and thermodynamic stability of this alloy in the different concentrations x=0.25, 0.5, and 0.75 in wurtzite phase. Moreover, we relied on the full-potential linearized augmented plane wave (FP-LAPW) as implanted byWien2K code. In section 2, we briefly describe the computational method used in the present work. Results will be presented in section 3. Finally, a brief summary and our conclusions are given in the ‘‘Conclusions’’ section 4.

2. Computational Details

The electronic configurations for **Mg, Se and Te, Mg: [Ne]$3s^2$, Se:[Ar]$3d^{10}4s^2$ 4p4** , and **Te:[Kr]$4d^{10}5s^25p4$**, respectively. All calculations were performed using the Vienna package WIEN2K **[33].** This is an implementation of a hybrid full-potential (linear) augmented plane-wave plus local orbitals (**L/APW + lo**) method within the density-functional theory. This new approach is shown to reproduce the accurate results of the **LAPW** method, but using a smaller basis set size. The APW + lomethod expands the Kohn–Sham orbitals in atomic like orbitals inside the atomic muffin-tin (**MT)** spheres and plane waves in the interstitial region. The details of the method have been described in literatures **[34-36].**We have used the Perdew–Burke–Ernzerhof generalized gradient approximation **[37]** (**PBE-GGA**). In addition, especially for electronic properties, we also applied the modified Becke–Johnson (**mBJ**) **[38, 39].**The self-consistent calculations are considered to be converged only when the calculated total energy of the crystal converged to less than **1 mRyd.** The choice of the particular (and different) muffin-tin (**MT**) radii for the various atoms in the compounds show small differences that do not affect our results. We have adopted the values of **2.2** ,**2.25**,**2.2** and **2.34ua**for **Mg, Se** and **Te,** respectively, as the MT radii.

The basis set inside each MT sphere is split into core and valence subsets. The core states are treated within the spherical part of the potential only and are assumed to have a spherically symmetric charge density totally confined inside the MT spheres. The valence part is treated within a potential expanded into spherical harmonics up to **l = 4**. The valence wave functions inside the spheres are expanded up to **l = 10**. A plane-wave expansion with RMT^*K_{MAX} equal to 8, and k sampling with a **4 x 4 x4 k**-points mesh in the full Brillouin zone turns out to be

satisfactory. The k integration over the Brillouin zone is performed using the Monkhorst and Pack mesh [40]. We compute lattice constants and bulk moduli by fitting the total energy versus volume according to the **Murnaghan's**equation of state [41].In addition, to investigate electronic and optical properties accurately, more k-points are needed and a denser **8 x 8 x 10 k** points are generated. Furthermore, the number of conduction bands is also an important parameter in the calculation, which defines the energy range covered and determines the accuracy of the Kramers–Kronig transform.

3. Resultes And Discussion

3.1. Structural Properties

In this section, we analyze the structural properties of the binary compounds **MgSe, MgTe** and their ternary alloys $MgSe_xTe_{1-x}$in the wurtzite structure using the PBE-GGA approximation. The alloys are modeled at some selected compositions with ordered structures described in terms of periodically repeated supercells. For the compositions **x = 0.25**, **0.5** and **0.75**, the simplest structure is an eight-atom simple wurtzite lattice. The total energies calculated as a function of unit cell volume are fitted to the **Murnaghan's** equation of state [41] to determine the ground state properties such as the equilibrium lattice constant **a**, **b** and **c** , the bulk modulus **B** and its pressure derivative **B′** . The corresponding equilibrium lattice constants and bulk modulus both for binary compounds and their alloys are given in **Table.1**. Considering the general trend that **PBE-GGA** usually overestimates the lattice parameters[42-48].our **PBE-GGA** results of binary compounds are in reasonable agreement with the experimental and other calculated values.

Table1. Lattice parameter a_0 and c_0, compressibility modulus B for the $MgSe_xTe_{1-x}$ alloy.

The Alloy	Concentrations	Lattice Parameters a (Å) c (Å)	Other calculations a (Å) c (Å)	Modulus of compressibility Our calcul Other calcul
$MgSe_xTe_{1-x}$ Wurtzite phase	0	4.617 7.494	4.61[a], 4.53[b], 7.48[a], 7.41[b], 7.38[c], 4.53[c], 4.55[d], 7.39[d], 7.39[e]	34.656 34.0[a], 38.0[c]
	0.25	4.589 7.434	4.54[e] - -	36.781 -
	0.5	4.443 7.197	- -	39.505 -
	0.75	4.321	-	41.237

	1	7.001 4.251 6.889	. - 4.28[a], 6.76[a], 6.98[f] 4.24[b], 6.84[b], 6.73[g] ,	- - 4.24[f], 4.15[g]	- 45.077 43.9[a], 50.8[f], 50.0[b]

[42][a], [43][b], [44][c], [45][d], [46][e],[47][f], [48][g]

The calculated lattice parameter at different compositions of $MgSe_xTe_{1-x}$ alloys exhibits tendency to Vegard's law **[49]** with a marginal upward bowing parameter equal to **–0.022** (a lattice parameter) and **-0.073** (c lattice parameter) Å**(Fig. 1).** The physical origin of the small deviation from the Vegard's law [49] should be mainly due to the weak mismatches of the lattice parameters of the binary compounds **MgSe** and **MgTe** . However, violation of Vegard's law has been reported in semi-conductor alloys both experimentally and theoretically **[42-48].** The overall behavior of the variation of the bulk modulus as a function of the composition x for $MgSe_xTe_{1-x}$ternary mixed crystals is presented in **Fig. 2**, and are compared to the results predicted by linear concentration dependence (LCD) method . A small deviation from LCD was observed with downward bowing equal to 1.352 GPa. However, this might be mainly due to the weak mismatch between the bulk modulus of the constitute binary compounds. A comparison of the lattice constant and bulk modulus of these alloys (Figs. 1 and 2) shows that an increase of the former parameter is accompanied by a decrease of the latter one, which is in agreement with the well-known relationship between the bulk modulus and the lattice constant: B $\propto V_0^{-1}$, where V_0 is the primitive cell volume**[50].**

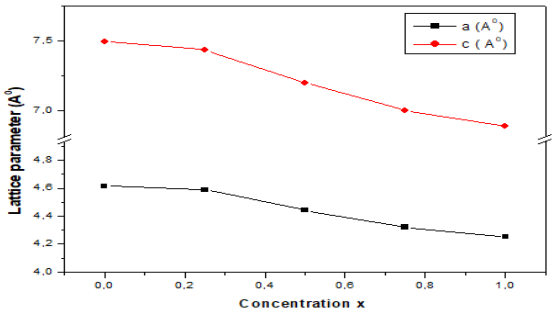

Figure1. Variation of the lattice parameter (a,c) as a function of the concentration x for the $MgSe_xTe_{1-x}$ alloy

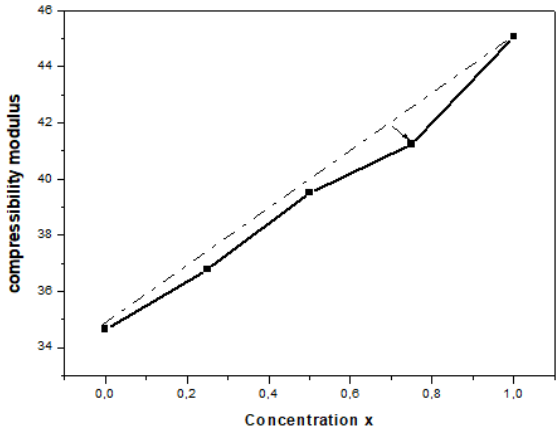

Figure 2. Variation of the Compressibility modulus as a function of the concentration x for the $MgSe_xTe_{1-x}$ alloy

3.2. Electronic Properties

The calculated band structures along the high symmetry directions of the $MgSe_xTe_{1-x}$ alloy with different concentration x are shown in **Fig.3 and Fig 4.** For **MgSe** and **MgTe**, the maximum of the valence band and the minimum of the conduction band locates at Γ point, showing it is a direct band gap semiconductor. It is obvious that other $MgSe_xTe_{1-x}$**(0, 0.25, 0.50, 0.75,1)** alloys also exhibit a direct band gap (**Γ-Γ**) character. Moreover, the band gap of all$MgSe_xTe_{1-x}$ shows an increasing feature varying with the molar fraction x.

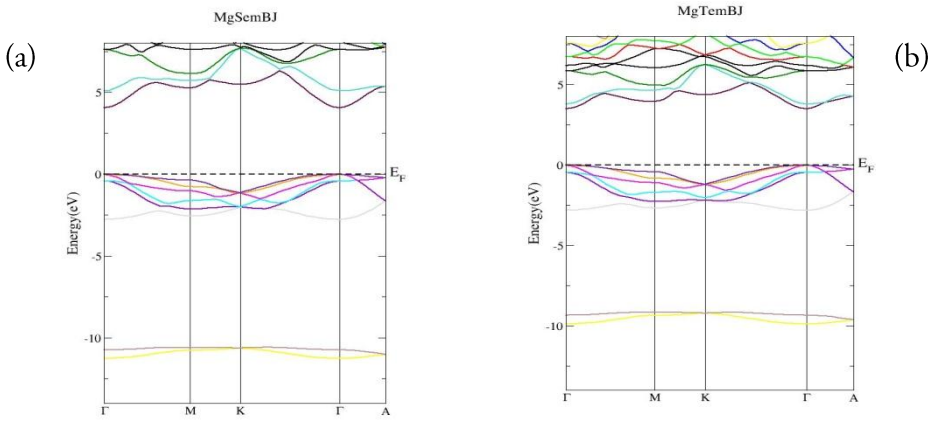

Figure 3. Calculated band structures for (a) MgTe and (b) MgSe along high symmetry directions in the Brillouin Zone

It is shown in **Table 2** that the calculated band gap for **MgSe ,MgTe** and ternary alloys $MgSe_xTe_{1-x.}$ our results and as a reference for other future works. From **Table 2,** we also note that the band gap energy decreases with increasing the composition x, which is due to the fact that the conduction bands shift to high energy. The disorder parameter of the alloy was

calculated by fitting the curve of the variation of the gap as a function of the concentration x(**Fig 5**) to a quadratic function, the gap takes the following form:

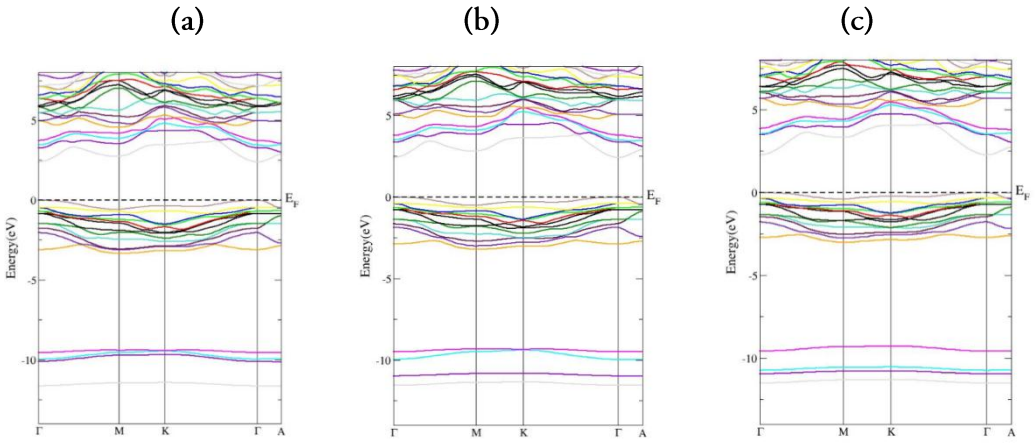

Figure 4. Calculated band structures for $MgSe_xTe_{1-x}$ alloys at x = 0.25 (a), 0.50 (b) and 0.75 (c) along high symmetry directions in the Brillouin zone

Table 2. Energy gaps of the $MgSe_xTe_{1-x}$ alloy calculated by the PBE-GGA and mBJ

The Alloy	Concentrations	Eg (eV) Γ-Γ PBE-GGa mBJ
$MgSe_xTe_{1-x}$ Wurtzite phase	0	1.961 2.504
	0.25	1.983 2.991
	0.5	2.05 3.076
	0.75	2.168 3.129
	1	2.310 3.227

$$MgSe_xTe_{1-x} \Rightarrow \begin{cases} E_g^{PBE-GGA} = 2.198 - 4.613x + 4.266x^2 \\ E_g^{mBJ-GGA} = 3.672 - 11.198x + 11.342x^2 \end{cases}$$

For a better understanding of the electronic structure of these materials and contribution of various states of the constituent atoms, we have calculated the total and partial density of states

(DOS) for the binary compounds and their ternary alloys in **Fig.6.** For the **MgTe** the valence band is composed of one region, is located at the energy range **[-2.868, 0.005] eV** which is formed by the hybridization of electrons from the s orbitals of **Mg** and p orbitals of **Te.** The conduction band is composed of a mixture of orbitalss, p and d of the two atoms. The second binary **MgSe** valence band is composed of one region, is located at the energy range **[-2.747, 0] eV** which is formed by the hybridization of electrons from the s, p orbitals of Mg and p orbitals of Se. The conduction band is composed of a mixture of orbitals s, p and d of the two atoms. For the $MgSe_xTe_{1-x}$ alloys and for each concentration **(x = 0.25, 0.5 and 0.75),** the lower valence band is composed of one region situated in the range **[-3.44, 0.0016] eV** is due to Mg-s, Mg-p mixed with **Se-p, Te-p**.The conduction band is due to **Mg-s, Mg-p** mixed with **Se-p, Se-d** and **Te-p, Te-d**. These figures show that these alloys have quite similar DOS.

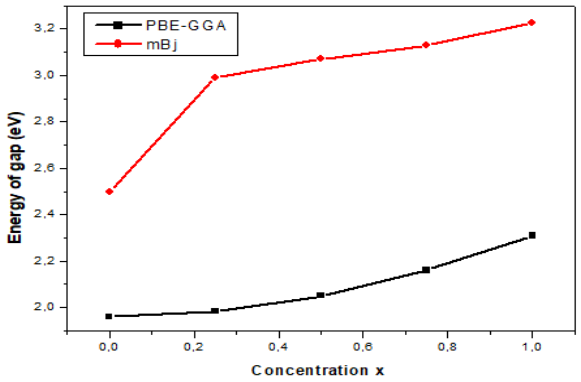

Figure 5. Variation of energy gaps as a function of concentration x for the $MgSe_xTe_{1-x}$ alloy, using PBE-GGA and mBJ

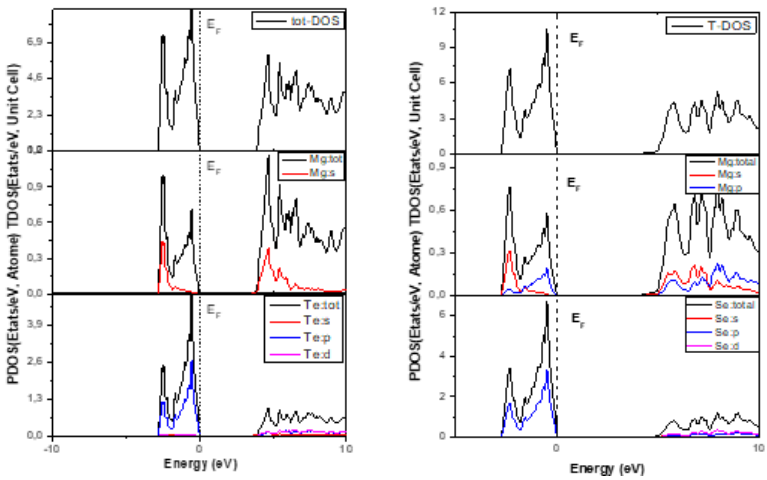

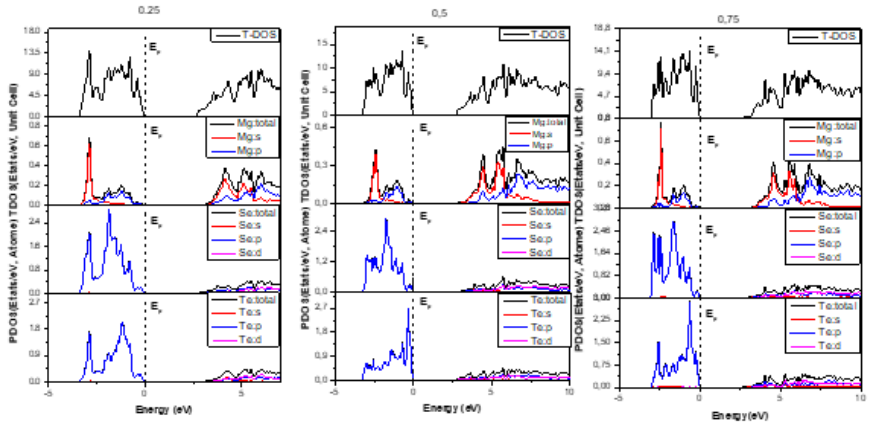

Figure 6. Calculated total and partial densities of states for the MgTe, MgSe and their $MgSe_xTe_{1-x}$ ternary alloys

3.3. Optical Properties

The optical properties of the material can be described by means of the complex dielectric function. The latter linearly relates the electric field **E (ω)** to the electric induction **D (ω)** by means of the following equation [51].

D

(E

For a dynamic field, ε (ω) corresponds to a complex function of the frequency of the electric field [52-55]:

$$\varepsilon(\omega) = \varepsilon_1(\omega) + i\varepsilon_2(\omega) \quad (2)$$

$\varepsilon_1(\omega)$: represents the real part of the polarization of the medium.

It is possible to extract the real and imaginary parts of the dielectric function using the kramers-kronig relations [56, 57]:

$$\varepsilon_1(\omega) = 1 + \frac{2}{\pi} P \int_0^{\infty} \frac{\omega' \varepsilon_2(\omega')}{(\omega'^2 - \omega_{12})} d\omega' \quad (3)$$

$$\varepsilon_2(\omega) = -\frac{2\omega}{\pi} P \int_0^{\infty} \frac{\varepsilon_1(\omega') - 1}{(\omega'^2 - \omega_{12})} d\omega' \quad (4)$$

P: being the principal value of the Cauchy integral. The complex refractive index, linked to the dielectric function **(ε)** will be to describe the medium; it is written on the format:

N (ω) = n (ω) + iK (ω). Ces deux grandeurs sont liées avec cette relation : $=N^2$.

The real and imaginary parts of the dielectric function are related to the refractive index (n) and the extinction coefficient (K) according to these formulas:

$$\varepsilon_1(\omega) = n^2 - K^2 \quad (5)$$

$$\varepsilon_2(\omega) = 2nK \quad (6)$$

The real refractive index n and the extinction coefficient K (losses) can be given by means of the following two relations **[58, 59]:**

$$n(\omega) = \left\{ \frac{\varepsilon_1(\omega)}{2} + \frac{\sqrt{\varepsilon_1^2(\omega)+\varepsilon_2^2(\omega)}}{2} \right\}^{\frac{1}{2}} \quad (7)$$

$$K(\omega) = \left\{ \frac{\sqrt{\varepsilon_1^2(\omega)+\varepsilon_2^2(\omega)}}{2} - \frac{\varepsilon_1(\omega)}{2} \right\}^{\frac{1}{2}} \quad (8)$$

Reflectivity is an important optical function calculated from the indices of refraction n (ω) and extinction K (ω):

$$R(\omega) = [(1-n)^2 + K^2]/[(1+n)^2 + K^2] \quad (9)$$

For low frequencies (ω = 0) relation (7) becomes:

$$n(0) =$$

Figures 7 illustrate the variations of the real and imaginary parts ($\varepsilon_1(\omega)$ and $\varepsilon_2(\omega)$) of the dielectric function as a function of energy for the ternary alloy **$MgSe_xTe_{1-x}$(x= 0-1).** We note considerable similarity between the spectra of **$MgSe_xTe_{1-x}$(x= 0-1),** with small differences in detail., we have two dielectric components; one, corresponding to the component of the electric field perpendicular to the c axis and the other, corresponding to that parallel to the X axis, beyond 30 eV no major difference between the components of the real and imaginary parts is observed, thus indicating that the compounds are isotropic in this energy range, even below this energy value the anisotropy is weak. Regarding the real part, the depth in the negative part for both compound **$MgSe_xTe_{1-x}$** is more pronounced than, hence the energy loss is greater in the x and z. The main peaks of the real part in the two directions are located at energies **(xx=4.42 eV** and **zz=4.73 eV), (xx= 4.35 eV** and **zz= 4.56 eV**), (**xx= 4.45eV** and **zz= 4.52 eV),(xx= 4.98 eV** and **zz= 4.99 eV**), and (**xx= 5.26 eV** and **zz= 5.55 eV),** for **$MgSe_xTe_{1-x}$x= 0, 0.25, 0.5,**

0.75 and **1**) respectively. The variation of the imaginary part $\varepsilon_2(\omega)$ of the dielectric function as a function of energy. This absorbing part represents a fundamental quantity of the optical properties of a material. Our analysis of the spectrum of $\varepsilon_2(\omega)$ shows that the critical points of $\varepsilon_2(\omega)$ occur at energies. **(xx=0.12 eV** and **zz=0.13 eV), (xx= 0.34 eV** and **zz= 0.35 eV**), (**xx= 0.61eV** and **zz=0.62 eV),(xx= 0.73 eV** and **zz= 0.74 eV**), and (**xx= 0.76 eV** and **zz= 0.77eV),** for $MgSe_xTe_{1-x}$**x= 0, 0.25, 0.5, 0.75** and **1**) respectively. These points correspond to the thresholds of the optical transitions between the top of the valence band and the bottom of the absorption conduction band, they represent the fundamental absorption thresholds. The values of the absorption thresholds correspond to the gaps obtained in the previous section. The different peaks observed in the spectra of the imaginary part correspond to direct optical transitions between the valence band and the conduction band.

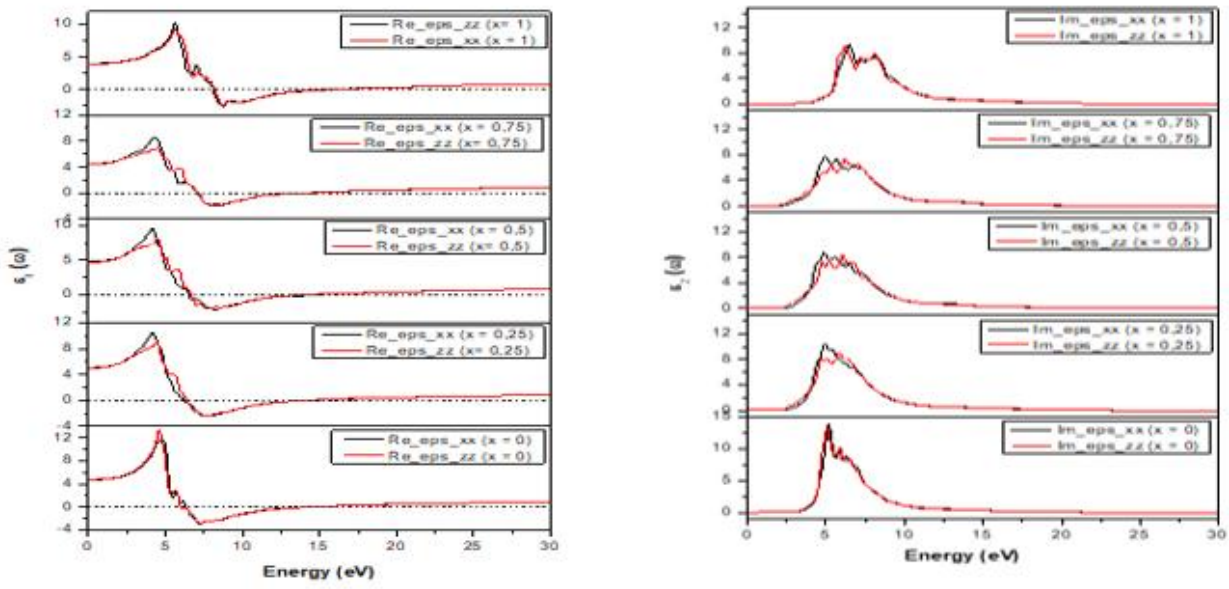

Figure7. Realε_1 (ω) and imaginary $\varepsilon_2(\omega)$ part of the dielectric function ε(ω) of the $MgSe_xTe_{1-x}$ ternary alloys: a) and b) hexagonal structure

The variation of the refractive index **n (ω)** and the extinction coefficient **k (ω)** as a function of energy is shown in **Fig 8**. From the spectrum the refractive index increases with the energy until it reaches a maximum value in the ultraviolet region for these alloys. The extinction coefficient **k(ω)** is related to the damping of the oscillation amplitude of the incident electric field. The maximum peak on the curve giving the extinction coefficient appears at the energy value where the dispersive part of the dielectric function has a zero value **(fig 8).** This is well verified for $MgSe_xTe_{1-x}$. Then, the extinction coefficient **k(ω)** decreases with increasing incident photon energy. The static value of ε_1 (ω), corresponding to a zero frequency, ie ε_1 (ω), is calculated. We have gathered the numerical results of ε_1 (ω) and also those of the static refractive index n**(ω)** and **k(ω)** obtained for our ternary alloy, as well as other theoretical data in **Table 3.** For the spectrum of energy loss which represents in **fig 9** the main peaks of the different concentrations

are not at the same energy. **MgTe(x = 0)** the main peak is located at (xx= **14.948 eV** and **zz= 14;961 eV)** , $MgSe_{0.25}Te_{0.75}$ (x = 0.25) it is located at(xx= **15.162 eV** and **zz= 15.183 eV),** $MgSe_{0.5}Te_{0.5}$ (x = 0.5) it is positioned at (xx=**15.171eV, zz= 15.194 eV)** is $MgSe_{0.75}Te_{0.25}$ (x = 0.75) it is located at (xx= **15.220 eV** and zz= 15.215eV) and **MgSe** (x = 1) it is located at (xx= **17.005 eV and zz= 17.123 eV).** These results are in agreement with the plasma oscillation frequencies$\varepsilon_p(\omega)$**.** Indeed, these peaks occur around the energies for which the imaginary part of the dielectric function reaches its minimum see **figure** 7 and the real part vanishes. The calculated optical reflectivity **R (ω)** is shown in **fig 9**

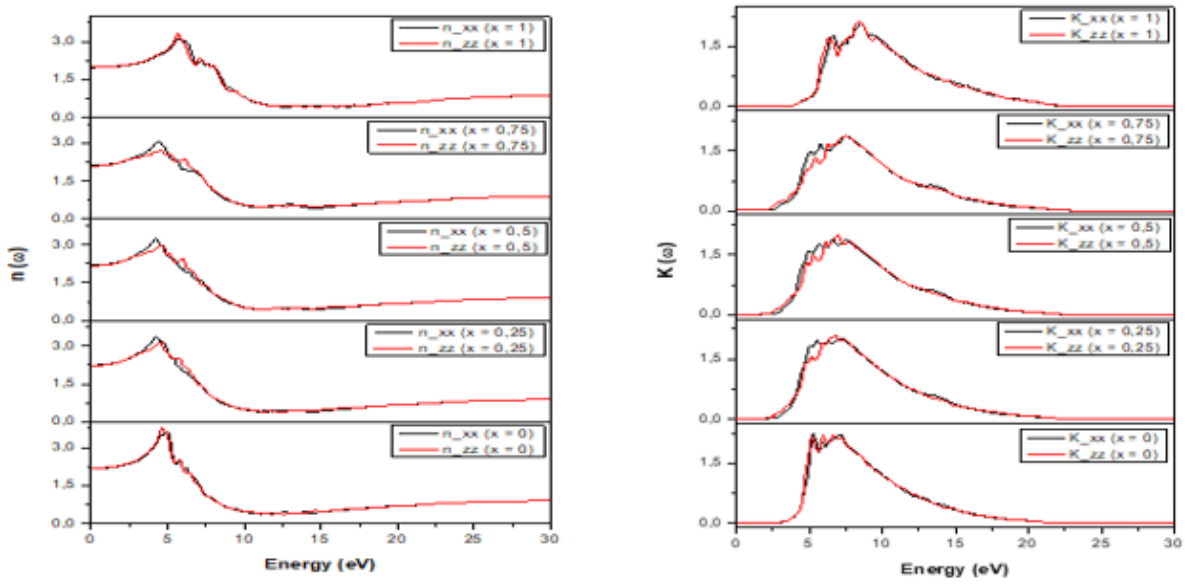

Figure 8. Refractive index n(ω) and extinction coefficient K(ω) of the $MgSe_xTe_{1-x}$ ternary alloys: (a), (b) hexagonal structure

Note that the maximum reflectivity occurs in the ultraviolet region of the electromagnetic spectrum, **(xx=15% and zz=16%), (xx= 13%** and **zz= 14%),** (**xx= 12%** and **zz=13%),(xx=11%** and **zz=12 %),** and (**xx= 9%** and **zz= 10%),** for $MgSe_xTe_{1-x}$**x= 0, 0.25, 0.5, 0.75** and **1**) respectively. The reflectivity decreases at high energies.

The absorption spectrum $\alpha(\omega)$ is shown in **Fig 10** for concentrations (x = 0, 0.25, 0.5, 0.75, 1) for radiation up to 30 eV. First, we can note that the curves have the same shape for all the concentrations. The threshold value of the absorption spectrum is

(xx=3.517eV and **zz=3.523 eV), (xx= 2.67eV** and **zz= 2.687 eV), (xx= 2.820 eV** and **zz=2.831 eV), (xx= 2.983 eV** and **zz= 2.995 eV)**and **(xx= 4.097eV** and **zz= 4.110eV),** for $MgSe_xTe_{1-x}$ **(x= 0, 0.25, 0.5, 0.75** and **1**) respectively . This value is close to the value of the energy gap.

Table 3.Values of the static dielectric constants ε_1 (0)the refractive index n (ω) and the extinction coefficient k (ω)

	$\varepsilon_1(0)$	n (0)	K(0)
The alloy $MgSe_xTe_{1-x}$	mBj	mBj	mBj
MgTe	ε_{xx1}= 4,719 ε_{zz1}=4.721	$n_{xx}(0)$= 2.173 $n_{zz}(0)$=2.183	$K_{xx}(0)$=0.005 $K_{zz}(0)$=0.006
$MgSe_{0.25}Te_{0.75}$	ε_{xx1}=4.819 ε_{zz1}=4.821	$n_{xx}(0)$= 2.244 $n_{zz}(0)$=2.252	$K_{xx}(0)$=0.098 $K_{zz}(0)$=0.099
$MgSe_{0.5}Te_{0.5}$	ε_{xx1}=4.859 ε_{zz1}=4.864	$n_{xx}(0)$= 2.267 $n_{zz}(0)$=2.276	$K_{xx}(0)$=0.105 $K_{zz}(0)$=0.106
$MgSe_{0.75}Te_{0.25}$	ε_{xx1}=4.872 ε_{zz1}=4.886	$n_{xx}(0)$= 2.298 $n_{zz}(0)$=2.307	$K_{xx}(0)$=0.146 $K_{zz}(0)$=0.150
MgSe	ε_{xx1}= 4.925 ε_{zz1}=4.934	$n_{xx}(0)$= 1.317 $n_{zz}(0)$=1.326	$K_{xx}(0)$=0.198 $K_{zz}(0)$=0.121

3.4. Thermodynamic Proprieties

In this part, we will study the phase stability of the MgSexTe1-x alloy by an ab-initio approach [60, 61].For this reason, we calculate the Gibbs free energy of the alloys, which provides access to the phase diagram and thus obtains the critical temperature Tc for the stability of the alloy.The Gibbs free energy for a mixture is given by the expression:

$$\Delta G_m = \Delta H_m - T\Delta S_m \quad (11)$$

Where

$$\Delta H_m = \Omega x(1-x) \quad (12)$$

$$\Delta S_m = -R[x\ln x + (1-x)\ln(1-x)] \quad (13)$$

ΔH_m and ΔS_m represent the enthalpy and entropy of the mixture respectively;Ω is the interaction parameter which depends on the considered material; R is the gas constant and T is the absolute temperature. The enthalpy of the alloys is obtained from the total energies calculated for the alloy and the parent binary compounds constituting this alloy. For an AB_xC_{1-x} alloy, the enthalpy ΔHm is given by:

$$\Delta H_m = E_{AB_xC_{1-x}} - xE_{AB} - (1-x)E_{AC} \quad (14)$$

From the expression, $\Omega = \Delta H_m / x(1-x)$, we can calculate the value of Ω for each concentration from the calculated enthalpies. By a linear fit of the curve Ω(x), the expressions of the interaction parameter Ω for the ternary alloy studied is given by the following equation:

$$MgSe_xTe_{1-x} \Rightarrow \Omega(kcal\ mol^{-1}) = 0.902x + 4.932 \quad (15)$$

The average value of Ω(x) in the concentration range 0≤x≤1, obtained from the equation for the alloy $MgSe_xTe_{1-x}$ and 5.383 kcal/mole.We calculate the free energy of the mixture ΔG_m for different concentrations using the equations, which will allow us to access the T-x phase diagram.The latter shows the stable, metastable and unstable regions of the alloy.At a temperature lower than the critical temperature TC, the binodal curve is determined for the temperatures verifying the relationship $\partial(\Delta G_m)/\partial x = 0$. The spinodal curve is obtained for temperatures obeying $\partial^2(\Delta G_m)/\partial x^2 = 0$.

The phase diagram obtained for the **$MgSe_xTe_{1-x}$**alloy is shown in the **fig 11**. The observed critical temperature is **2386.87 K**. The spinodal curve in the phase diagram marks the equilibrium solubility limit, ie, the gap is miscibility. For temperatures above the spinodal curve, a homogeneous alloy is predicted. The metastable phase is predicted for temperatures lying between the spinodal and binodal curves. Finally, our results indicate that this alloy is stable at high temperature.

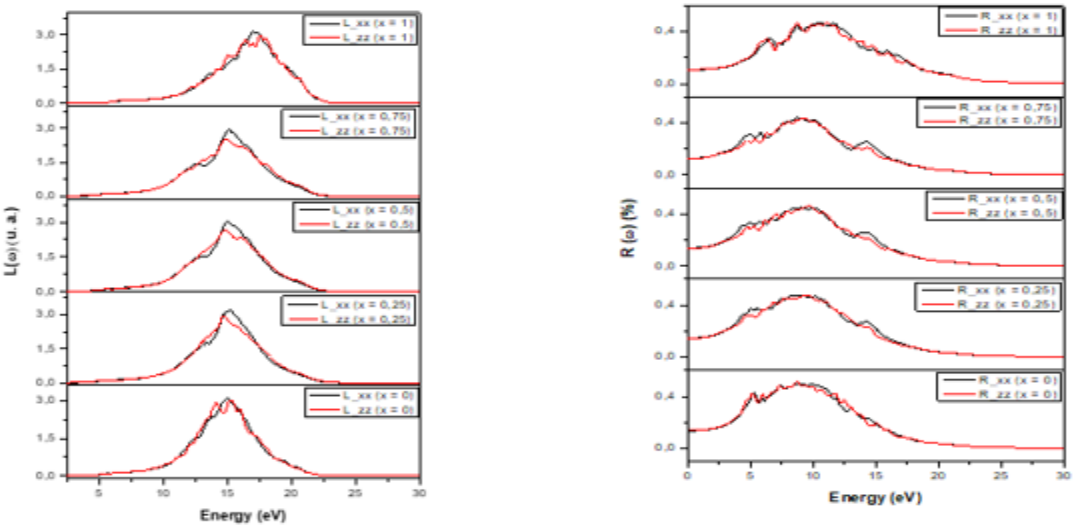

Figure9.Function of electron energy loss L(ω) and reflectivity R(ω) of $MgSe_xTe_{1-x}$ ternary alloys: a), b) hexagonal phase

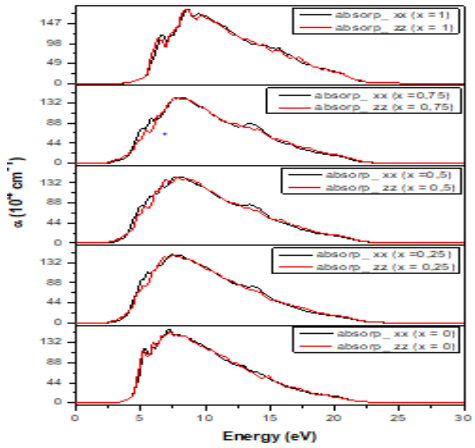

Figure10.The variation of the absorption coefficient as a function of energy for $MgSe_xTe_{1-x}$ ternary alloys

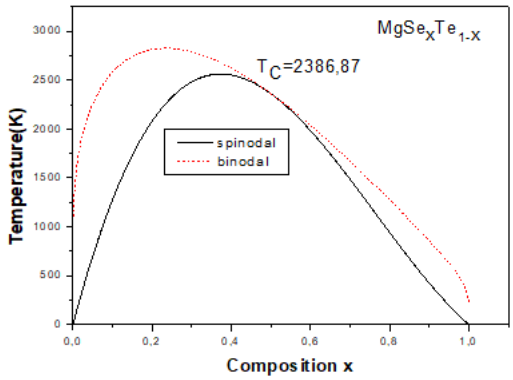

Figure 11.T-x phase diagram of the $MgSe_xTe_{1-x}$ alloy (dotted line: binodal curve, solid line: spinodal curve)

4. Conclusion

During this work, we studied the structural, electronic, optical and thermodynamic properties of the ternary alloy $\mathbf{MgSe_xTe_{1-x}}$, a composition ranging from 0 to 1 in steps of 0.25. The calculations were carried out by the method ab-initio called augmented plane waves (FP-LAPW) as part of the theory density functional (DFT).

- The structural results such as the lattice parameter and the compressibility modulus are in good agreement with the theoretical and experimental values available in the literature.
- The study of the structures of the electronic bands allowed us to conclude that the gap for the compounds **MgTe** and **MgSe** and their ternary alloy $\mathbf{MgSe_xTe_{1-X}}$ are direct. The calculated values of the gaps of these compounds using (PBE-GGA) and (mBj) correspond well to the theoretical data.
- The most interesting for a semiconductor is the optical properties. We have determined the complex dielectric function and the refractive index. The results obtained are in good agreement with those of other theoretical calculations.
- We determined the thermodynamic properties of this alloy using Debye's quasi-harmonic model. Our results can serve as references for future investigations on these materials.

References

[1] M. W. Wang et al, ”n-CdSe/p-ZnTe based wide band-gap light emitters: Numerical simulation and design ‘’, J. Appl. Phys. 73, 4660 (1993). doi: 0021-8979/93/094660-09$06.00

[2] R. Pandey and S. Sivaraman, ’’Spectroscopic properties of defects in alkaline-earth sulfides’’, J. Phys. Chem. Solids 52, 211 (1991). Doi: https://doi.org/10.1016/0022-3697(91)90066-9

[3] D. J. Chadi, ‘’Doping in ZnSe, ZnTe, MgSe, and MgTe wide-band-gap semiconductors’’, Phys. Rev. Lett. 72, 534 (1994). Doi:https://doi.org/10.1103/PhysRevLett.72.534

[4] X. Liu et al, ’’Optical properties of epitaxial ZnMnTe and ZnMgTe films for a wide range of alloy compositions’’, J. Appl. Phys. 91, 2859 (2002).Doi: https://doi.org/10.1063/1.1448402

[5] A Sajid, SM Alay-e-Abbas, A Afaq,”STRUCTURAL, ELECTRONIC AND OPTICAL PROPERTIES OF MgSxSe1-x, MgSxTe1-x AND MgSexTe1-x (0 ≤x ≤1) ALLOYS FROM FIRST PRINCIPLES’’, International Journal of Modern Physics B Vol. 26, No. 17- 1250098 (2012). Doi: 10.1088/0004-637X/735/1/43

[6] H.Okuyama et al.,'' Epitaxial growth of ZnMgSSe on GaAs substrate by molecular beam epitaxy'',J. Cryst. Growth 117, 139 (1992). https://doi.org/10.1016/0022-0248(92)90727-Z
[7] M. A. Hasse et al.,Optical gain of CdZnSe/ZnSe quantum well lasers,Appl. Phys. Lett. 59, 1272 (1991). Doi: https://doi.org/10.1063/1.105472
[8] S. Albin et al., " Stimulated electronic transition concept for an erasable optical memory'', J pn. J. Appl. Phys. 31, 715 (1992). Doi : 10.1143/JJAP.31.715
[9] S. H. Wei and A. Zunger, ''Role of metal d states in II-VI semiconductors'', Phys. Rev. B 37, 8958 (1988) Doi : https://doi.org/10.1103/PhysRevB.37.8958
[10] J Guo, A Sarikhani, P Ghosh, T Heitmann, YS Hor, "Chemically induced ferromagnetism near room temperature in single crystal (Zn 1– x Cr x) Te half-metal'', RSC ADV, 13, 8551-8556 (2023).Doi : 10.1039/D2RA08105A
[11] B. Khalfallah• F. DrissKhodja • B. Doumi • M. Berber • A. Mokaddem • A. Bentayeb, ''Theoretical study of structural, electronic and optical properties of novel ternary alloys (0.25, 0.50 and 0.75)'', Journal of Computational Electronic, 018-1188 (2018). Doi:10.1007/s10825-018-1188-7
[12] El Akkad, F., Demian, S. & Chevallier Photoluminescence and optical properties of Mg x Zn1–x Te alloys, J Mater Sci 20, 165 (1985) Doi : https://doi.org/10.1007/BF00555909
[13] H. Okuyama, Y. Kishita, and A. Ishibashi, "Quaternary alloy Zn 1– x Mg x Se", Phys. Rev. B 57, 2257 (1998). Doi:https://doi.org/10.1103/PhysRevB.57.2257
[14] F El Haj Hassan and B Amrani, "Structural, electronic and thermodynamic properties of magnesium chalcogenide ternary alloys'', Journal of Physics: Condensed Matter, 19, 38(2007) Doi: 10.1088/0953-8984/19/38/386234
[15] A. L. Ruoff et al.,"Sevenfold coordinated MgSe: experimental internal atom position determination to 146 GPa, diffraction studies to 202 GPa, and theoretical studies to 500 GPa", Phys. Rev. Lett. 81, 2723 (1998). Doi :https://doi.org/10.1103/PhysRevLett.81.1774
[16] Ebru Begeç, Sıtkı Eker and Süleyman Bozdemir, "Russian Reactivity of fluoroalkanes in reactions of coordinated molecular decomposition ", Journal of Physical Chemistry A . 91, 1408 (2017). Doi: 10.1134/S003602441708009X
[17] W. Zachariasen, Z. Über, "die Kristall struktur des Magnesium tellurids , Phys. Chem. 128, 417 (1927). Doi : https://doi.org/10.1016/0022-1902(69)80141-7
[18] W. Klemm and K. Wahl, Z. Anorg, Notiz über das Magnesiumtellurid'', Allg. Chem. 266, 289 (1951). Doi:90c33c7e26f7c04d59fc266b6121e8c6
[19] A. Kuhn, A. Chevy and M.-J. Naud, "Preparation and some physical properties of magnesium telluride single crystals'' , J. Cryst. Growth. 9, 263 (1971). Doi : 10.1149/1.2408236

[20] J.C. Guillaume, J. Chevallier, J.F. Rommeluere, G. Rouy et G. Revel, '' Conditions de croissance et luminescence des alliages Zn1-xMg xTe'', Phys. Appl. 11, 725 (1976). DOI: 10.1051/rphysap:01976001106072500

[21] A.Waag et al. ''Growth of MgTe and Cd1– xMgxTe thin films by molecular beam epitaxy'', J. Cryst. Growth. 131, 607 (1993). Doi: https://doi.org/10.1016/0022-0248(93)90213-G

[22] T. Li et al., ''High pressure phase of MgTe: Stable structure at STP''; Phys. Rev. Lett. 74, 5232 (1995).
Doi: 10.1103/PhysRevLett.74.5232

[23] G.Gokoglu, M. Durandurdu and O. Gulseren, ''First principles study of structural phase stability of wide-gap semiconductors MgTe, MgS and MgSe ''; Comp. Mat. Sci. 47, 593 (2009).
Doi: https://doi.org/10.1016/j.commatsci.2009.09.029

[24] F.Drief et al., ''First principles study of structural, electronic, elastic and optical properties of MgS, MgSe and MgTe'', Catal. Today, 89, 343 (2004). Doi: https://doi.org/10.1016/j.cattod.2003.12.013

[25] Dong-Ho Shin , Chang-Dae Kim , Hyang-Hee Jang , Sung-Hyu Choe , Duck-Tae Kim , Chang-Sun Yoon , Wha-Tek Kim, ''Growth and characterization of MgxCd1 – xSe single crystals'', Journal of Crystal Growth, 177, 1–2, 167 (1997). Doi: https://doi.org/10.1016/S0022-0248(97)00122-X

[26] Yanbing Han, Hanyu Zhang, Tursun Ablekim, Imran Khan, Kristin A. ''Persson and AndriyZakutayev'',ChemRev. 120, 9, 4007 (2020). Doi: https://doi.org/10.1021/acs.chemrev.9b00600

[27] F El Haj Hassan and B Amrani, ''A study of the surface structure of deposited Au on Pb film''; J. Phys.: Condens. Matter. 19, 386234 (2007). Doi: https://doi.org/10.1016/j.physb.2006.11.046.

[28] Y. Megdoudet al, ''Ab-initio study of the physical properties of Zn1-xMgxSeyTe1-yquaternary alloy'', EuroQuantology, 21 (6) 1416 (2023). Doi : 10.48047/nq.2023.21.6.NQ23144

[29] S. Duman et al. ''First-principles studies of ground-state and dynamical properties of MgS, MgSe, and MgTe in the rocksalt, zinc blende, wurtzite, and nickel arsenide phases'', Phys. Rev. B 73, 205201 (2006).
Doi : 10.1103/PhysRevB.73.205201

[30] A. Shaukat et al, ''Ab initio study of structural, electronic and optical properties ternary alloy'',Physica B 404, 3964 (2009). Doi : 10.1016/j.physb.2009.07.147

[31] A. Amin, I. Ahmed and M. Maqbool, ''STRUCTURAL, ELECTRONIC AND OPTICAL PROPERTIES OF MgS x Se 1–x , MgS x Te 1–x AND MgSe x Te 1–x (0 ≤ x ≤ 1) ALLOYS FROM FIRST PRINCIPLES'' Light. Wav. Tech. 28, 223 (2010). Doi : https://opg.optica.org/jlt/abstract.cfm?URI=jlt-28-24-3497

[32] L. Tairi et al, ''Phase stability and electronic behavior of MgS, MgSe and MgTe compounds, Phase Transitions'', 90(10), 929 (2017). Doi: https://doi.org/10.1080/01411594.2017.1302085
[33] P.Blaha, K. Schwarz, G. K. H. Madsen, D. Kvasnicka and J. Luitz, ''WIEN2K, an augmented plane wave + local orbitals program for calculating crystal properties'', Techn. Universitat, Wien, ISBN 3-9501031 (2001). doi: 10.1038/s41598-022-26250-7
[34] E. Sjostedt, L. Nordstrom, D.J. Singh, ''An alternative way of linearizing the augmented plane-wave method'', Solid State Commun. 114, 15 (2000). Doi: https://doi.org/10.1016/S0038-1098(99)00577-3
[35] G.K.H. Madsen, P. Blaha, K. Schwars, E. Sjostedt, L. Nordstrom,'' Efficient linearization of the augmented plane-wave method'' ,Phys. Rev. B 64 195134 (2001). Doi : https://doi.org/10.1103/PhysRevB.64.195134
[36] K. Schwarz, P. Blaha, G.K.H. Madsen, ''Electronic structure calculations of solids using the WIEN2k package for material sciences'', Comput. Phys. Commun. 147, 71(2002). Doi: https://doi.org/10.1016/S0010-4655(02)00206-0
[37] P. Perdew, S. Burke, M. Ernzerhof, ''Generalized Gradient Approximation Made Simple'', Phys. Rev. Lett. 77, 3865 (1996). Doi:https://doi.org/10.1103/PhysRevLett.77.3865
[38] F. Tran and P. Blaha, ''Accurate band gaps of semiconductors and insulators with a semi local exchange-correlation potential''. Phys. Rev. Lett. 102, 226401 (2009). Doi : 10.1103/PhysRevLett.102.226401
[39] D. Becke and E. R. Johnson, "A simple effective potential for exchange", J. Chem. Phys. 124, 221101 (2006). Doi ; https://doi.org/10.1063/1.2213970
[40] H.J. Monkhorst, J.D. Pack, ''Special Points for Brillouin-Zone'' IntegrationsPhys. Rev. B 13,5188 (1976). Doi:https://doi.org/10.1103/PhysRevB.13.5188
[41] F.D. Murnaghan, Proc. Natl. Acad. "The Compressibility of Media under Extreme Pressures'',
Sci. USA 30, 5390 (1944). Doi: https://doi.org/10.1073/pnas.30.9.244
[42] BIMAL DEBNATH, MANISH DEBBARMA, DEBANKITA GHOSH, SAYANTIKA CHANDA, RAHUL BHATTACHARJEE and SURYA CHATTOPADHYAYA ,''Structural, mechanical and optoelectronic properties of cubic BexMg1−xS,BexMg1−xSe and BexMg1−xTe semiconductor ternary alloys: a density functional study'', Bull. Mater. Sci. 43, 59 (2020). Doi: https://doi.org/10.1007/s12034-019-2006-y
[43] Van Camp PE, Van Doren VE, Martins JL.''High Pressure Phases of Magnesium Selenide and Magnesium Telluride".Phys.Rev.B.;55, 775 (1997). Doi : https://doi.org/10.1103/PhysRevB.55.5799
[44] M. D. Johannes et al. ''Fermi-surface nesting and the origin of the charge-density wave'', Phys.Rev B. 73, 205 (2006). Doi : https://doi.org/10.1103/PhysRevB.73.205205
[45] Li T, Luo H, Greene RG, et al.'' Observation of the Top Quark'', Phys. Rev. Lett. 74, 5232 (1995). Doi:https://doi.org/10.1103/PhysRevLett.74.2632

[46] Pengfei Yu, ,Biru Jiang, Yongren Chen, Jiahong Zheng, and Lijun Luan, ''Study on In-Doped CdMgTe Crystals Grown by a Modified Vertical Bridgman Method Using the ACRT Technique'', Materials (Basel).12, 4236 (2019). Doi : 10.3390/ma12244236
[47] Rached D, Benkhetto N, Soudini B, et al. ''Predictions of Electronic, Transport, and Structural Properties of Magnesium Sulfide (MgS) in the Rocksalt Structure'', Phys Stat Sol (b). 240, 565 (2003). Doi ; https://doi.org/10.1002/pssb.200301889
[48] Mittendorf H et al . ''Röntgenographische und optische Untersuchungen aufgedampfter Schichten aus Erdalkalichalkogeniden'', Z Phys. 183, 113 (1965). Doi : 10.1007/BF02457136
[49] L. Vegard.''Ab Initio Study of Structural and Electronic Properties of Barium Chalcogenide Alloys Z''. Phys. 5,17 (1921). Doi: https://doi.org/10.1007/BF01327675
[50] M. L. Cohen, ''Calculation of bulk moduli of diamond and zinc-blende'', solids Phys. Rev. B 32, 7988 (1985). Doi:https://doi.org/10.1103/PhysRevB.32.7988.
[51] F. Bassani, G. Pastroi, Parravicini, ''Electronic States and Optical Transitions in Solids'', Pergamon Press, Oxford, (1973). Doi:10.1007/978-3-662-07150-2_1.
[52] J.S. Tell, Bremsstrahlung,'' Polarization Measurements for 1.0-Mev Electrons'' , Phys. Rev. 104,1760 (1956). Doi:https://doi.org/10.1103/PhysRev.104.626.
[53] L.D. Landau, E.M. Lifshitz, ''Electrodynamics in Continuous Media'', Pergamon Press, Oxford (1960).Doi: 9780750626347.
[54] H.A. Kramers, ''Collected Science Papers'', North Holland, Amsterdam, 333. (1956) Doi: https://doi.org/10.1121/1.429586.
[55] R.De.L. Kronïg, ''Polarized single-crystal specular reflectance spectra in the visible and ultraviolet'',
[56] J. Opt. Soc. Am. 12, 547 (1926), Doi: https://doi.org/10.1016/0038-1098(87)90860-X.
C. A. Draxl, R. Abt, ''Theoretical study of the electronic structure, chemical bonding and optical properties the paraelectric cubic phase'', ICTP lecture notes, unpublished, (1998). Doi : 10.1088/0953-8984/15/35/304.
[57] P. Y. Yu, M. Cardona, "Fundamentals of Semiconductors'', Physics and Materials Properties. Berlin: Springer-Verlag, 233. (2010). Doi: 10.1007/978-3-642-13884-3.
[58] S. M. Hosseini, "Optical properties of cadmium telluride in zinc-blende and wurzite structure",
[59] ,Physica B 403, 1907 (2008). Doi: https://doi.org/10.1016/j.physb.2007.10.370.
[60] D. Lee, A.M. Johnson, J.E. Zucker, C.A. Burrus, R.D. Feldman, R.F.Austin, ''Optical Constants of Zn1-xCdxTe Ternary Alloys: Experiment and Modeling'', IEEE Photon. Technol. Lett. 4, 949 (1992).
Doi: DOI 10.1143/JJAP.32.3496.
[61] R.A. Swalin, R.A. Swalin, "Thermodynamics of Solids, Phase Diagrams and Heterogeneous Equilibria'', J. Wiley, New York, NY, (1972). Doi: 10.1007/978-3-662-09276-7_6

[62] L.G. Ferreira, S.-H. Wei, A. Zunger,''First-principles calculation of alloy phase diagrams: The renormalized-interaction approach'', Phys. Rev. B 40, 3197 (1989). Doi:https://doi.org/10.1103/PhysRevB.40.3197

[63] L. Teles, J. Furthmüller, L. Scolfaro, J. Leite, F. Bechstedt, ''First-principles calculations of the thermodynamic and structural properties of strained alloys'', Phys. Rev. B 62, 2475 (2000).
Doi : https://doi.org/10.1103/PhysRevB.62.2475.